JOURNAL OF MATERIALS SCIENCE 26 (1991) 1640–1646

Crack propagation in brittle materials under compressive stresses studied by caustics

P. S. THEOCARIS, M. SAKELLARIOU
Department of Engineering Sciences, Athens National Technical University, PO Box 77230, Athens 17510, Greece

An experimental study was undertaken concerning the propagation of a slant crack under compression. By using the equations of the deformed shape of a crack and by introducing a correction model in order to prevent the crack lips from incompatible displacements, an estimate of the stress distribution along the crack borders was achieved. It was found that an opening-mode K_I stress intensity factor (SIF) must be introduced at the crack tips in the overall compressive stress field, in order to give the required space for the *lip-slip* phenomenon, due to shearing, to take place. This local dilatation in the vicinity of the crack tip, together with the lip-slip phenomenon, due to which the initial crack tip is displaced into a new position along the deformed crack borders, causes the out-of-plane propagation of the crack, either towards the largest compressive stress in the case of biaxial stress field, or towards the applied compression in a uniaxial compressive field. A series of experiments on PMMA (perspex) rectangular specimens with pre-existed cracks and slits has been executed and the type of the stress field in the front of the propagated branches is examined by using the method of caustics. It was found that the crack propagation under compression is an interactive process of two conjugate branches, which is strongly influenced by the boundary conditions of the pre-existed discontinuity.

1. Introduction

The problem of crack propagation under compression has been extensively examined, because of its importance in rock fracture as well as in tectonic processes in the earth's crust [1–12]. In formulating the problem of a crack embedded in a compressed body, as is usually the case in rock mechanics, a difficulty is faced concerning the boundary conditions along the crack lips.

So far, two approaches have been adopted. According to the first approach we can resolve the far field stresses along the direction of the crack posing the condition, that at the crack tips the mode-I K_I-SIF must have a zero-value whereas, because of the interaction of the crack lips, a frictional shear strength must be developed obeying Coulomb's law expressed by

$$\tau = c + \sigma \tan \varphi$$

where τ is the shear strength, σ is the normal stress on the crack direction, $\tan \varphi$ is the coefficient of friction and c is the cohesion coefficient [2, 9, 12].

According to the second approach a condition related to the kinematics of the problem is assumed. The condition is that along the crack lips the displacements in a direction normal to the crack axis for the upper and lower lips must be equal [4, 10, 13].

By examining the displacement field, which corresponds to the above-mentioned approaches of the solution, it can be shown that for both solutions it is not compatible with the necessary condition, that an interpenetration of the crack lips must be avoided. Indeed, the exact solution of the displacement field of a crack loaded biaxially has shown that, the presence of shear stresses in a direction parallel to the crack causes the angular displacement of the initial crack axis [14]. In the case under consideration, where the crack is embedded in a compressive stress field, this rotation of the crack axis due to loading causes the interpenetration of the crack lips forming a *negative* ellipse according to the exact analytical solution of the problem [15]. Thus, an additional compressive stress distributed along the crack borders must be present to revoke the incompatible displacements. In this way the coupling of the crack borders under compression and shear causes the development of compressive stresses, which are larger than those corresponding to the crack direction due to a far-field compression. This "*internal pressure*" must be taken under consideration when dealing with crack initiation and crack propagation criteria in elastic materials.

In order to overcome this coupling of the crack borders in many theoretical and experimental studies the model of an "*open crack*" has been used [2, 7, 8, 11].

In this paper a model has been introduced for the approximate calculation of a uniformly distributed stress acting on the crack borders, which resulted in compatible displacements of the crack lips. After examining the influence of this stress on the direction of

0022–2461/91 $03.00 + .12

the crack initiation, the crack propagation process under compression has been experimentally studied using the method of caustics [16–18].

2. Theoretical background

Theocaris *et al.* [14], using the solution given by Muskhelishvili [19] to the problem of an internal crack in an infinite plate subjected to a biaxial loading, have found that the displacement field of the deformed shape of the crack is determined by:

$$\begin{pmatrix} u \\ v \end{pmatrix} = \frac{\sigma_\infty(\kappa + 1)}{8G} \begin{pmatrix} \{(1 - k)(\sin 2\beta)x \pm [(1 + k) - (1 - k)\cos 2\beta]\sqrt{(\alpha^2 - x^2)}\} \\ \{(1 - k)(\cos 2\beta)x \pm [(1 - k)\sin 2\beta]\sqrt{(\alpha^2 - x^2)}\} \end{pmatrix} \quad (1)$$

where

$$c = \sigma_\infty(\kappa + 1)/8G = \begin{cases} \sigma_\infty/E \text{ for plane stress} \\ \sigma_\infty(1 - \nu^2)/E \text{ for plane strain} \end{cases}$$

α is the semi-length of the crack axis, β the angle between the main loading axis and the crack axis, κ the Muskhelishvili coefficient, k the biaxiality factor, G the shear modulus, E the elastic modulus of the material and ν the Poisson ratio. The plus-sign holds for the upper crack border, whereas the minus-sign holds for the lower crack border.

By using the expressions for the SIFs K_I and K_{II} [20], where K_{II} expresses the shear mode SIF, and by defining the dimensionless SIFs N_I and N_{II} by the relations:

$$N_I = \frac{K_I}{\sigma_\infty(\pi\alpha)^{1/2}}, \qquad N_{II} = \frac{K_{II}}{\sigma_\infty(\pi\alpha)^{1/2}} \quad (2)$$

Equation 1 becomes:

$$\begin{bmatrix} u^\pm \\ v^\pm \end{bmatrix} = 2c \begin{bmatrix} \left(\frac{1 + k}{2} - N_I\right) \cdot x \pm N_{II}(\alpha^2 - x^2)^{1/2} \\ \pm N_I(\alpha^2 - x^2)^{1/2} + N_{II}x \end{bmatrix} \quad (3)$$

By defining, further that:

$$[u] = (u_+ - u_-) \text{ and } [v] = (v_+ - v_-) \quad (4)$$

from Equation 3 we get:

$$\begin{bmatrix} u \\ v \end{bmatrix} = 4c(\alpha^2 - x^2)^{1/2} \begin{bmatrix} N_{II} \\ N_I \end{bmatrix} \quad (5)$$

From Equation 5 we may conclude that the above-mentioned two approaches, when dealing with compressed cracks, i.e. either $[v] = 0$ or $K_I = 0$, are identical.

It was found in [14] that the deformed shape of the crack borders is, in general, elliptical with its major and minor axes given by [14]:

$$\begin{bmatrix} \alpha_1 \\ \alpha_2 \end{bmatrix} = \frac{1 + c(1 + k)}{2}\alpha \pm 1/2\alpha\{[1 - c(1 + k)]^2 + 4c(1 - k)[1 - c(1 + k)]\cos 2\beta + 4c^2(1 - k)^2\}^{1/2} \quad (6)$$

where the plus sign corresponds to α_1 and the minus one to α_2.

When the crack is under a uniaxial loading, the minor axis, α_2, is always negative and the boundary conditions of the problem must be changed, so that the crack remains at least straight and there is no overlapping of its flanks.

As a first approximation to this problem we may superimpose a uniformly distributed stress along the borders of the "negative" ellipse, in order to revoke the incompatible displacements. To do this we may calculate the amount of stress to be superimposed along the flanks of the crack in order to make its minor axis to become equal to zero.

It has been shown [21] that a crack loaded by an internal pressure p, is being deformed to an ellipse, whose shape is determined by the transverse displacements, v_x given by [18]:

$$v_x = 2c(\alpha^2 - x^2)^{1/2} \quad (7)$$

By solving the inverse problem we can calculate the necessary dimensionless stress c' by the equation:

$$c' = \frac{v_{(0)}}{2\alpha} \quad (8)$$

where $v_{(0)}$ is the particular v-displacement of the flanks of the crack for $x = 0$, which expresses the semi-length of the minor axis of the "negative" ellipse given by Equation 6, c' is a displacement coefficient, which corresponds to the stresses along the crack borders, and α is the initial semi-length of the crack.

The so calculated coefficient c' is greater than the normal to the crack axis dimensionless stress ($c \sin^2\beta$), which corresponds to the case of the far field stress, determined by the coefficient c.

This excess in the value of c', determined by the difference ($c' - c \sin^2\beta$), corresponds to the additional compressive stress which is developed along the crack lips, due to the shearing.

In Fig. 1 the quantity $(c' - c\sin^2\beta)/c$ is plotted against the angle β of slantness of the crack for different c-values. From this figure we can observe that the extra value of compression follows a pattern similar to the shear stresses corresponding to the crack orientation. Indeed, it has a maximum value for $\beta = 45°$ and vanishes for $\beta = 0°$ and 90°. For exceedingly large c-values, e.g. $|c| \geqslant 0.250$, we have a departure from linearity and the maximum occurs for lower angles than $\beta = 45°$.

In order to estimate the influence of the coupling of the crack lips on the orientation of the crack propagation, the following procedure has been adopted. By using the displacement discontinuity method based program MINAP [13], we can calculate the stresses at the vicinity of the crack tips for different boundary conditions.

We have used two types of discontinuities. The first assumed stress-free borders, thus modelling the slit

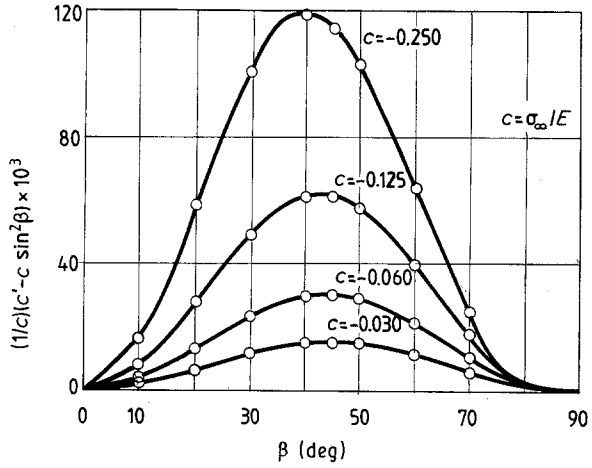

Figure 1 The variation of the dimensionless stress $(1/c)$ $(c' - c \sin^2 \beta)$ due to shearing for $\beta = 0°$ to 90°.

case, and the second accepted distributed compressive stresses according to the above analysis, thus modelling the crack case.

As the present analysis is an approximate solution of the problem, we have selected the more simple method in order to estimate the angle θ of the initiation of the crack propagation. By calculating the total energy along a circle with its centre at either crack tip we made an estimation of the initial angle according to the S-criterion for simplicity [22]. Thus, we have found a strong influence of the boundary conditions of the model, on the value of the angle, θ, of crack propagation.

Table I contains the so calculated θ-values for stress-free borders, thus simulating the slit case and for compressed borders as in the crack case. We can observe from Table I that the interaction of the crack lips results in a reduction of the angle θ whereas in the case of stress-free lips we obtain θ-values even larger than $\theta = 90°$.

3. Experimental study

In order to experimentally study the crack propagation phenomenon under compression, we have selected two particular problems: the first was the type of the stress field developed near the front of a propagated crack and the second was the detailed study of the geometry of the branches of a stationary crack. Both problems are essential in back-analysis studies, in order to testify the validity of the proposed crack-initiation and crack-propagation criteria.

TABLE I The values of the angle of kinking, $\theta°$, versus the angle $\beta°$, for the slit and crack cases ($c = -0.250$)

$\beta(°)$	$\theta(°)$	
	The slit case stress-free borders	The crack case compressed borders
15	45	52
30	68	57
45	90	65
60	107	62
75	113	75

The specimens used were made by polymethylmethacrylate (PMMA) and they had rectangular shapes. The load was applied by an Instron testing machine with a capacity of 50 kN. The first specimen, whose dimensions were: height $H = 0.1$ m and thickness $d = 0.009$ m, was slotted at a length $BB' = 0.021$ m (Fig. 2a). This initial slit was extended at both its ends by a wedge action, thus forming two collinear cracks AB and A'B' (Fig. 2a). The orientation of the slit, with its extensions, with the respect to the loading axis of the specimen was $\beta = 45°$.

The respective configuration for the second specimen, whose dimensions were: height $H = 0.098$ m, length $L = 0.096$ m and thickness $d = 0.01$ m, is also, indicated in Fig. 2b.

To estimate the type of the stress field at the crack tips, the experimental method of caustics has been used [16–18]. According to this method a coherent light beam impinges on the specimen and its reflections from the front and rear faces of the specimen, as well as those transmitted through its thickness light rays, are received on reference screens. As the thickness of the specimen and its refractive index are strongly influenced by the high stress concentration, which is developed at the close vicinity of the crack tips, the reflected or transmitted light rays deviate forming a singular epicycloidal curve on the reference screen, which is called caustic. It has been shown [23], that by measuring any diameter of the caustic and the angle of inclination of the axis of symmetry of the caustic relative to the crack axis, we can calculate the SIF-components K_I and K_{II}. In the present study a He–Ne Laser has been used as the light source and the

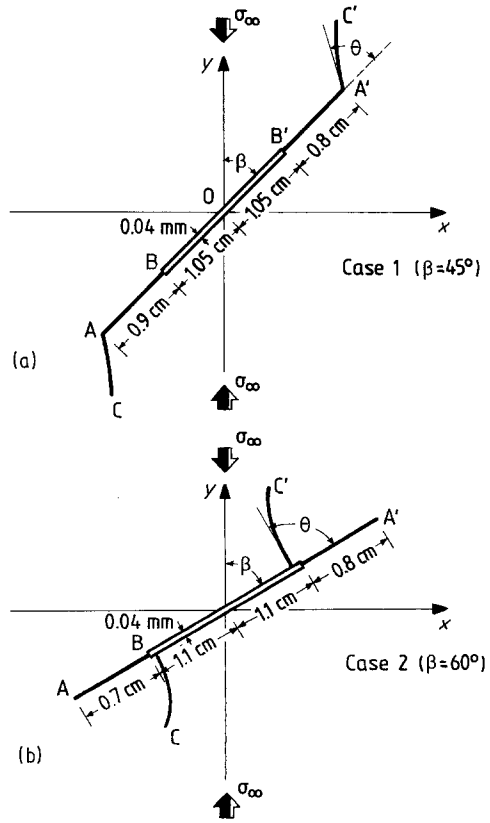

Figure 2 The configuration of the two specimens used in the experimental study.

so obtained caustics have been recorded on a video tape recorder.

3.1. The $\beta = 45°$ specimen

In Fig. 3a and b the reflected caustics from both faces of the specimen at the extremities of the pre-existing cracks and the initial slit are shown for two loading steps, whereas in Fig. 4a and b the caustics at two steps of the propagation are given. The experimental arrangement, which was used, did not permit a real time recording of the load applied. The whole process was stable, as an increased load was necessary for further propagation to take place. The load at which

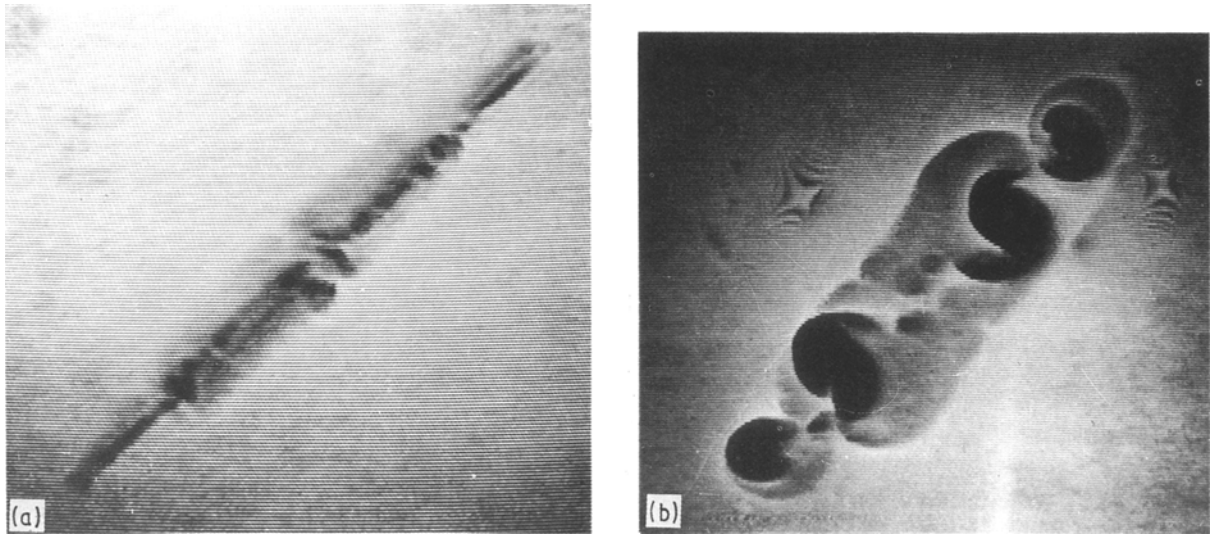

Figure 3 The reflected caustics of the pre-existed slit and cracks under compression. (a) Before loading, (b) under loading ($\beta = 45°$).

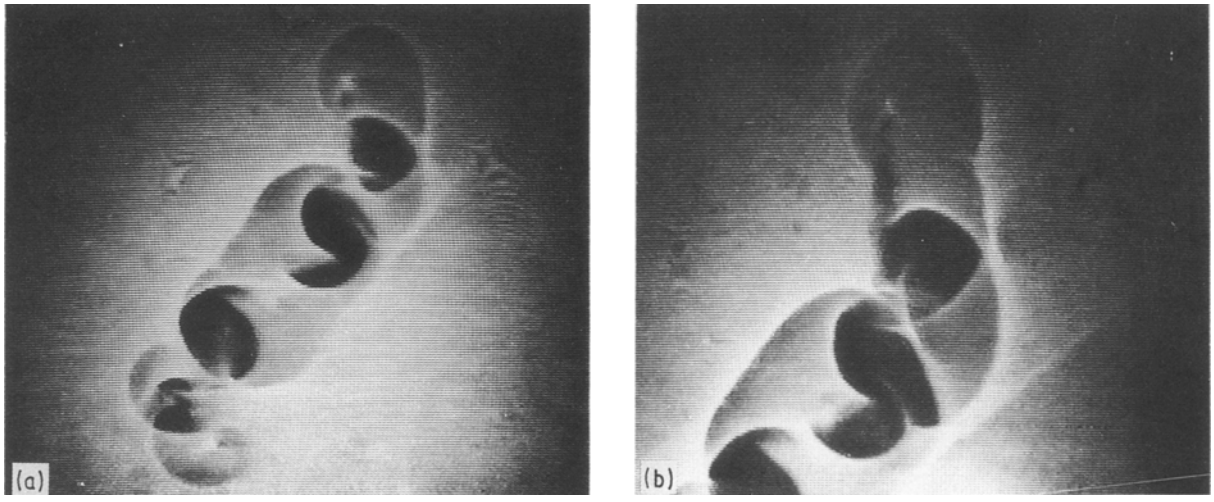

Figure 4 The reflected caustics at the tip of the propagated branch. (a) First step, (b) final step ($\beta = 45°$).

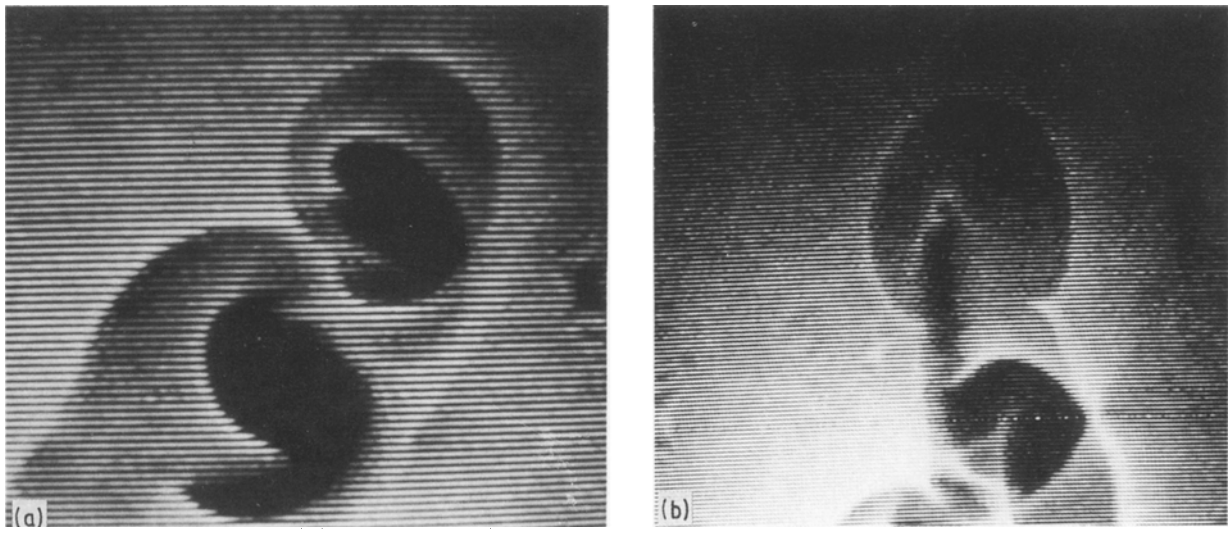

Figure 5 Details of the caustics: (a) before kinking and (b) after kinking ($\beta = 45°$).

TABLE II The relative coordinates of characteristic points of the branches of the $\beta = 45°$ specimen

Branch a (A′ C′) (Number of steps: 6)					Branch b (AC) (Number of steps: 7)				
Step	ΔX (mm)	ΔY (mm)	D (mm)	$\theta(°)$	Step	ΔX (mm)	ΔY (mm)	D (mm)	$\theta(°)$
(A′ − 1)	− 0.953	3.015	3.162	63	(A − 1)	0.911	− 2.506	2.666	65
(1 − 2)	− 0.812	1.742	1.922	70	(1 − 2)	0.557	− 1.680	1.770	63
(2 − 3)	− 1.192	5.217	5.352	58	(2 − 3)	0.650	− 3.477	3.537	56
(3 − 4)	− 0.695	3.537	3.605	56	(3 − 4)	0.630	− 4.195	4.242	54
(4 − 5)	− 0.544	3.626	3.667	54	(4 − 5)	0.728	− 5.319	5.368	53
(5 − C′)	− 1.654	5.520	5.762	62	(5 − 6)	0.253	− 2.457	2.470	51
					(6 − C)	0.545	− 1.381	1.484	67

we had the initiation of the propagation was $P = 20$ kN. In Fig. 5a, a magnification of the caustic developed at the tip of the initial crack, before kinking is presented. By examining its inclination, we may conclude, that it is a K_{II}-caustic with its outer branch almost circular [18]. In Fig. 5b, the caustic at the tip of the branch after a step of propagation is presented. This caustic is a mixed-mode one, with a positive K_I SIF, as its axis of symmetry does not coincide with the path of the propagation. This means that at the tip of the propagated crack, a mixed-mode type stress field was present.

As far as the geometry of the propagation is concerned, the following remarks have been done. The initiation of the crack propagation occurred at the vicinity of the tip A′ of the crack B′ A′. In this way, in the experiment under consideration a crack propagation from an initial real crack took place.

After the first step of the kinking took place, a second anti-symmetric branch initiated from the vicinity of the other tip A of the real crack AB for almost constant load. Thus, the propagation was a step by step process, in which each step of the first branch preceded always of each step of the opposite branch of the propagating crack.

By inspecting the traces of the two branches we have observed that, each step of the first branch was always rougher than each step of the second one with an "*en-echelon*" texture. We have also observed that the surfaces of the branches were curved along the thickness of the specimens and were almost normal to the specimen surfaces.

The geometry of the two branches is given analytically in Table II, as it is obtained via a digitizer, whereas Fig. 6 presents the traces of the branches based on the above values.

We can derive from Table II and Fig. 6, that in the last observed step of propagation a change in the orientation of the direction of the branches of the propagation took place. This was because this final step took place during the unloading process of the specimen due to the recovering of a part of the energy imposed on the specimen.

3.2. The $\beta = 60°$ specimen

Contrary to what happened in the $\beta = 45°$ specimen, in the secondary experiment with $\beta = 60°$ the initiation of the propagation started at the vicinity of the

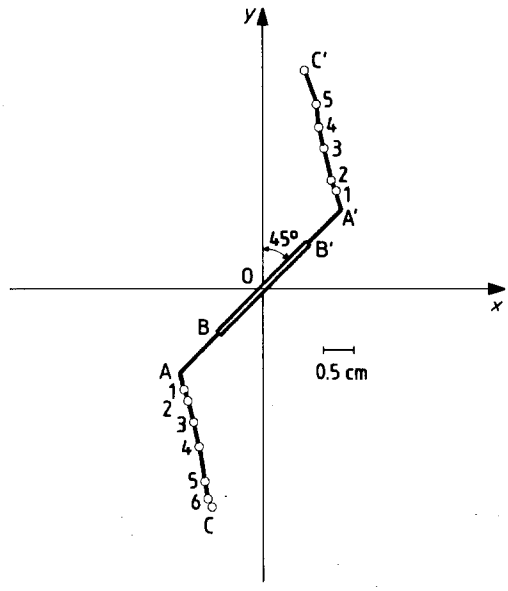

Figure 6 The final configuration of the $\beta = 45°$ specimen.

extremities of the pre-existing slit and not at the tips of the extended real cracks. In this case the branches formed almost right angles to the slit borders.

As in the first experiment we have observed, that the propagation process involves two propagated step-by-step branches, with a delay of each second relatively to the respective kink of the first branch. We have also observed that, as in the first experiment each first branch was relatively rougher than the respective second branch and that the surfaces of the branches were, again, curved normally to the plate surfaces.

A series of transmitted caustics is presented in Fig. 7. From these caustics we can follow the whole process of the propagation of branches. Thus, in Fig. 7a to c we can see the interaction of the two branches, as the initiation of the first branch resulted in an increasing of the size of the caustics of the other extremity of the slit, thus triggering the initiation of the respective second branch.

In Fig. 7d we can observe the interaction of the two branches. Again, as the second branch initiated, the caustic of the first branch changed its direction. In Fig. 7e and f the caustics of the propagated branches are given from which we can establish that they have almost the same orientation and magnitude. This identity in the mode of propagation of branches means that the stress field at the tips of the two antisymmetric branches is of the same type irrespective of their differences in time and geometry.

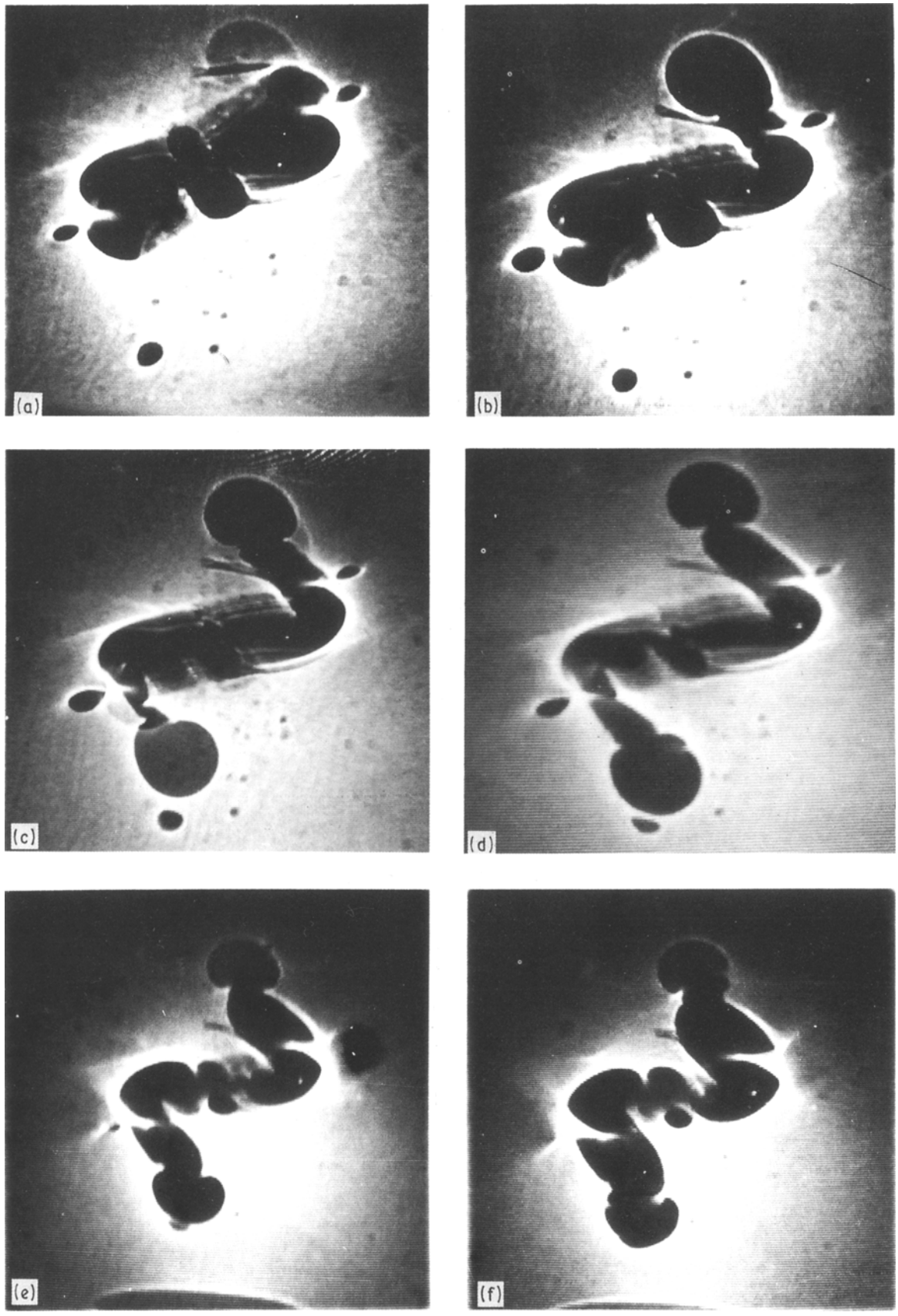

Figure 7 The transmitted caustics of the pre-existed discontinuity and of the propagated branches at successive steps ($\beta = 60°$).

By comparing the inclination of the caustics relatively to the axes of the traces of the branches we may conclude that, as in the previous experiment, the stress fields at the tips of the branches are of the mixed-mode type with a positive opening-mode K_I SIF.

The digitized branches are given in Table III, whereas in Fig. 8 the so analysed branches have been plotted. By inspecting the two antisymmetric branches we have found that, the interaction of the two branches, observed in Fig. 7d, correspond to a bifurcation

TABLE III The relative coordinates of characteristic points of the branches of the $\beta = 60°$ specimen

Branch a (B′ C′) (Number of steps: 7)					Branch b (BC) (Number of steps: 5)				
Step	ΔX (mm)	ΔY (mm)	D (mm)	$\theta(°)$	Step	ΔX (mm)	ΔY (mm)	D (mm)	$\theta(°)$
(B′ – 1)	– 1.681	1.538	2.279	108	(B – 1)	0.920	– 1.129	1.457	99
(1 – 2)	– 0.412	1.066	1.142	81	(1 – 2)	1.754	– 5.406	7.198	101
(2 – 3)	– 2.066	4.400	4.861	85	(2 – 3)	1.151	– 2.507	2.759	85
(3 – 4)	– 1.023	1.489	1.806	94	(3 – 4)	0.388	– 2.353	2.384	69
(4 – 5)	– 0.096	1.378	1.381	64	(4 – C)	– 0.973	– 6.684	6.755	52
(5 – 6)	0.684	1.522	1.669	36					
(6 – C′)	– 0.188	3.175	3.180	63					

of the first initiated branch, changing in this manner the direction of its propagation (Fig. 8). Finally, in Table III and Fig. 8 it can be observed that, as in the first experiment, a change in the orientation of the propagation took place during the unloading of the specimen.

4. Conclusions

An estimation of the stresses along the crack borders, necessary to prevent any incompatible displacements, has been established. By using the results of this approximate solution, the influence of the boundary conditions of the crack lips was studied. It was found, that the interaction of the crack lips resulted in smaller angles of crack intiation than in the slit case, where the crack borders are stress free.

From the experimental study reported in this paper we may conclude that:

1. The propagation of a discontinuity, crack or slit, under compression involves two conjugated branches with a time delay between them and a relatively rougher trace of the firstly initiated branch.

2. The stress field at the tips of the propagated branches is of the same type, as it is concluded from the recorded caustics.

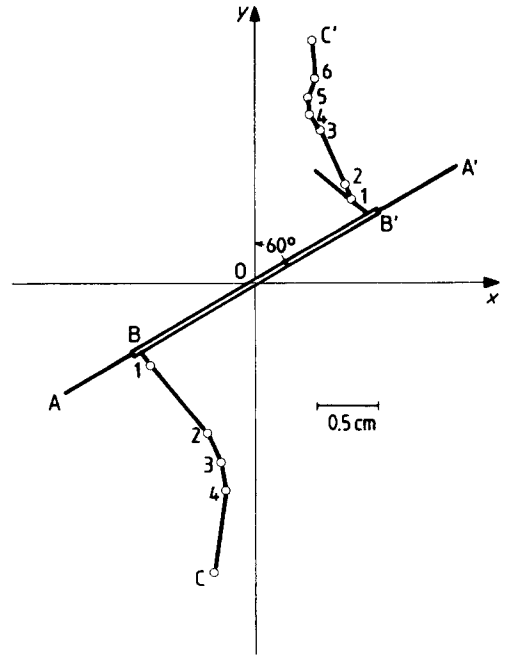

Figure 8 The final configuration of the $\beta = 60°$ specimen.

From the above arguement we may conclude that, in analysing the crack propagation under compression process, we must have in mind the interaction of the two branches, as well as the influence of the boundary conditions of any pre-existed discontinuity.

References

1. E. G. BOMBOLAKIS, *Tectonophysics* **1** (1964) 343.
2. E. HOEK, "Rock fracture under static conditions", National Mechanical Engineering Research Institute, C.S.I.R., Pretoria, Report MEG 383 (1965).
3. E. HOEK and Z. T. BIENIAWSKI, *Int. J. Fract. Mech.* **1** (1965) 137.
4. G. P. CHEREPANOV, *PMM* **30** (1966) 82.
5. Z. T. BIENIAWSKI, *Int. J. Rock Mech. Min. Sci.* **4** (1967) 395.
6. W. F. BRACE and E. G. BOMBOLAKIS, *J. Geophys. Res.* **68** (1963) 3709.
7. S. A. F. MURRELL, *Br. J. Appl. Phys.* **15** (1964) 1195.
8. B. COTTERELL, *Int. J. Fract. Mech.* **8** (1972) 195.
9. F. ERDOGAN, "Continuum Mechanic Aspects of Geodynamic and Rock Fracture Mechanics", Proc., NATO Advance Study Inst. edited by P. Thof-Christensen (D. Reidel Publications, Holland, 1974) p. 45.
10. S. NEMAT-NASSER and H. HORII, *Int. J. Engng Sci.* **22** (1984) 999.
11. A. R. INGRAFFEA, in "Fracture Mechanics of Rock", edited by B. K. Atkinson (Academic Press, London, 1987) p. 71.
12. V. LI, *ibid.* p. 351.
13. S. L. CROUCH, "Analysis of Stresses and Displacements around Underground Excavations: An Application of the Displacement Discontinuity Method", Geomechanics report to the National Science Foundation, University of Minnesota, USA (1976).
14. P. S. THEOCARIS, D. PAZIS and B. KONSTANTELLOS, *Int. J. Fracture* **30** (1986) 135.
15. P. S. THEOCARIS, *Engng Fract. Mech.* **26** (1986) 753.
16. *Idem., Appl. Optics* **10** (1971) 2240.
17. *Idem.*, in "Developments in Stress Analysis" I, edited by G. S. Holister (Applied Science Publishers, London, 1979).
18. *Idem.*, in "Mechanics of Fracture" Vol. 7, edited by G. C. Sih (Nijhoff Publications, The Hague, 1981) Ch. 3, p. 189.
19. N. I. MUSKHELISHVILI, "Some Basic Problems of the Mathematical Theory of Elasticity" (Noordhoff International, Leyden, 1975).
20. P. C. PARIS and G. C. SIH, in "Fracture Toughness Testing and its Applications", ASTM, STP 381 (1969) p. 30.
21. A. E. GREEN and W. ZERNA, "Theoretical Elasticity" (Oxford University Press, London, 1968).
22. G. C. SIH, in "Methods of Analysis and Solutions of Crack Problems" edited by G. C. Sih (Noordhoff International, Leyden, 1973) p. 21.
23. P. S. THEOCARIS and D. PAZIS, *Appl. Optics* **20** (1981) 4009.

Received 8 November
and accepted 1 December 1989